

Machining of complex-shaped parts with guidance curves

Laurent Tapie · Bernardin Mawussi · Walter Rubio ·
Benoît Furet

Received: 21 December 2012 / Accepted: 5 June 2013 / Published online: 26 June 2013
© Springer-Verlag London 2013

Abstract Nowadays, high-speed machining is usually used for production of hardened material parts with complex shapes such as dies and molds. In such parts, tool paths generated for bottom machining feature with the conventional parallel plane strategy induced many feed rate reductions, especially when boundaries of the feature have a lot of curvatures and are not parallel. Several machining experiments on hardened material lead to the conclusion that a tool path implying stable cutting conditions might guarantee a better part surface integrity. To ensure this stability, the shape machined must be decomposed when conventional strategies are not suitable. In this paper, an experimental approach based on high-speed performance simulation is conducted on a master bottom machining feature in order to highlight the influence of the curvatures towards a suitable decomposition of machining area. The decomposition is achieved through the construction of intermediate curves between the closed boundaries of the feature. These intermediate curves are used as guidance curve for the tool paths generation with an alternative machining strategy called “guidance curve strategy”. For the construction of intermediate curves, key parameters reflecting the influence of their

proximity with each closed boundary and the influence of the curvatures of this latter are introduced. Based on the results, a method for defining guidance curves in four steps is proposed.

Keywords CAM · Machining strategies · Guidance curves · Complex-shaped parts

1 Introduction

High-speed machining (HSM) production of hardened material parts with complex shapes such as dies and molds is an economical process. Indeed, part production is faster for better quality and longer fatigue life for the parts, but the cutting process induces the use of specific machining techniques and technologies [1, 2]. Moreover, tasks carried out during the preparation step are mainly based on computer-aided machining (CAM) software that provides several machining strategies (<http://www.delcam.com>) (<http://www.mastercam.com>). Selection of these strategies is a very complex task. Indeed, several parameters in different fields (quality, cost, geometry ...) should be considered during machining strategy selection and tool paths generation. Besides, commercial CAM solutions with relevant assistance modules for machining strategies selection are scant [3, 4].

HSM cutting characteristics stand for one of the main topics difficult to integrate in CAM software. Unfortunately, HSM cutting phenomenon has a direct influence on part surface integrity [5]. Importance of integrating the characteristics and impacts of the HSM in tool paths generation is therefore critical for complex shaped parts [6]. The correlation between part's topology (shape, size and local curvature of mold, and die features for example), cutting tool types, cutting parameters (depths of cut, cutting speed, and feed rate), and machining strategies (machining direction, sweeping direction) has been underlined in several works [7, 8]. Some studies on surface integrity after hard milling of mold and die (hardened steel) highlight the links between part surface residual

L. Tapie · B. Mawussi
Unité de Recherches Biomatériaux Innovants et
Interfaces—URB2i, Université Paris Descartes, EA4462,
1 Rue Maurice Arnoux,
92120 Montrouge, France

L. Tapie (✉) · B. Mawussi
IUT de Saint Denis, Université Paris 13, Place du 8 mai 1945,
93206 Saint Denis Cedex, France
e-mail: laurent.tapie@univ-paris13.fr

W. Rubio
Université de Toulouse, Institut Clément Ader,
UPS, 118, route de Narbonne,
31062 Toulouse, France

B. Furet
Institut de Recherche en Communications et Cybernetique de
Nantes (IRCCyN), UMR CNRS 6597, 1 rue de la Noe, BP92101,
44321 Nantes Cedex 3, France

stress, effective cutting speed, effective feed rate and contact area of tool/part [9–11]. Parameters defining machining strategies are also relevant factors for obtaining surface integrity. The residual normal stresses along feed and step over directions increased with the radial depth of cut and feed rate increase [12]. For the works presented in this paper, only the topology of the parts, the cutting conditions, and the machining strategy were retained in the experimental study.

A tool path implying stable cutting conditions might guarantee a better part surface integrity. To ensure this stability, the shape machined must be decomposed when conventional strategies are not suitable. In this paper, experiments are carried out in order to analyze the influence of the decomposition. Machining performance simulated during the decomposition process is evaluated towards feed rate reductions (main criteria), machining time, and tool path lengths. A bottom feature extracted from complex forging dies is the shape considered because it cannot be machined easily with conventional machining strategies such as parallel planes. First, the experimental setups including a module for high-speed performance (HSP) evaluation are presented. Then, the decomposition method is detailed through the construction of the intermediate curves and machining areas. Finally, the analysis of the results leads to the proposal of a first definition of guidance curves.

2 Experimental setup

2.1 Experimental machining feature

The machining feature studied in this work is a typical forging die machining feature called “bottom feature.” According to the definition developed in previous works

[13, 14], a bottom feature is generally in contact with two flanks in order to form a cavity (Fig. 1a, b). In general, such cavity comes out in other cavities on each opened boundary. Due to its own basic geometry and the topology of its relationship with flanks, a bottom feature may induce more or less complex machining tool paths.

The master bottom feature presented in this paper (Fig. 1c) is in contact with flanks along two edges very curved and nonparallel in order to study their influence on the machining tool paths. Besides, the topology of this master bottom feature is much curved.

2.2 Guidance curve machining strategy

Traditionally, a machining assistant uses standard three axes parallel planes strategy widely available in CAM software for the machining of bottom features [15, 16]. A key characteristic of this machining strategy at the finishing stage is that the parallel planes contain the tool axis, which also defines the machining feed direction (Fig. 2a). The basic direction of the parallel planes is defined from the opened sides of the bottom feature. This basic direction can be adjusted according to topological information defined in the bottom machining feature model [13, 14].

Analysis and simulation of the tool paths generated for the feature presented in Fig. 2 show that the feed rate set point is not reached on the whole surface of the bottom feature (Fig. 2b). Three types of feed rate reductions can be distinguished. Feed rate reductions induced by small curvature radii defined in the CAD model of the feature (type 1). This type of feed rate reduction can be deleted, only if the geometry of the feature is modified in the CAD model. Feed rate reductions closed to opened boundaries of the bottom feature (type 2) can be avoided, if the tool paths are extended

Fig. 1 Bottom features and experimental machining feature

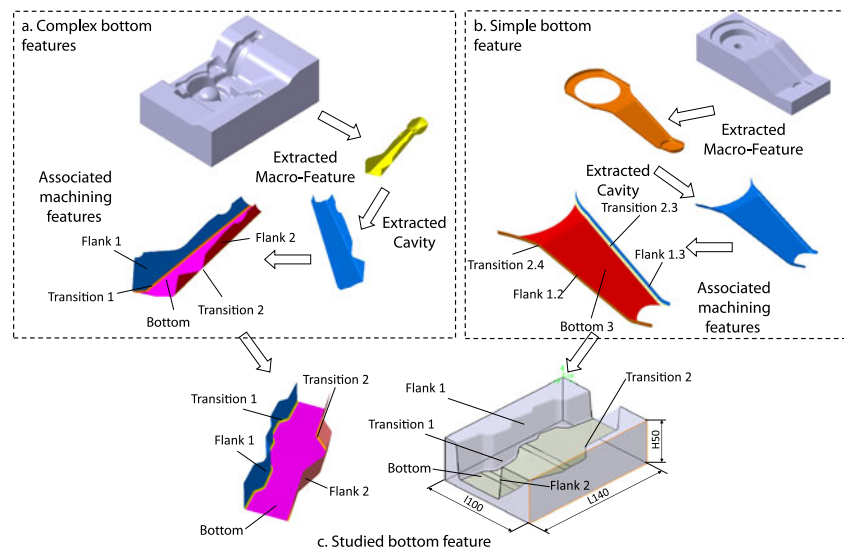
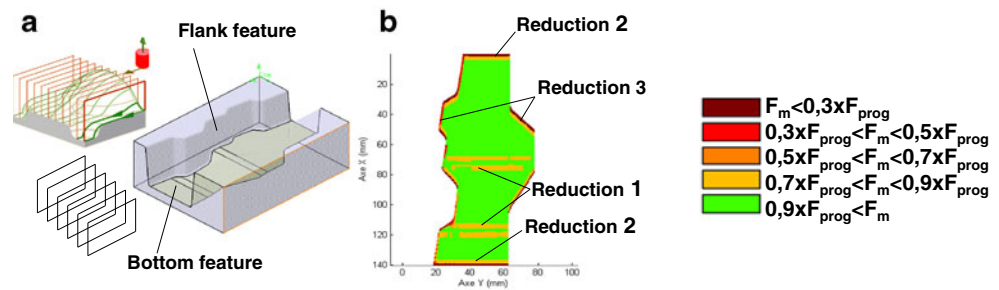


Fig. 2 Parallel planes tool path analysis



over the boundaries. Flank features induced feed rate reductions (type 3) because their intersections with the bottom feature are not straight and parallel lines. This type of feed rate reductions, which mainly correspond to tool entrance/exit, can be partially avoided by choosing another machining strategy, which is more closed to the topology of the bottom feature. Machining strategies must be chosen appropriately in order to avoid feed rate reductions and tool entrances/exits because they have an impact on roughness and the part surface integrity (local crack, local hardness variations). Parallel plane strategy used for the example presented in Fig. 1 is relevant for the central area of the bottom feature, whereas along the limits of flank features, it is not relevant according to feed rate analysis.

An alternative machining strategy should be chosen or developed for processing these constraints induced by the flank features, which have a particular topology. In this paper, an alternative strategy, called “guidance curve” strategy, is studied. This work is carried out on tool paths computation using the guidance curves strategy implemented on the CAM software CATIA® V5. The implementation of this strategy requires first the definition of two guidance curves (Fig. 3), and then the generation of tool paths by morphing between these two guides curves.

2.3 High-speed performance evaluation

Machining time and geometrical allowance of parts are the main components of HSP. In this work, HSP is evaluated by the tool paths analysis: ISO block extracted from the machining program sent to the machine tool are analyzed according to its length and the mean value of the simulated feed rate reached compared with the set point. The HSP is evaluated using the “performance viewer” module (Fig. 4a). The feed rate

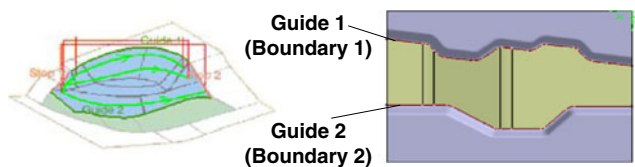


Fig. 3 Guidance curves strategy

simulation principle is detailed on Fig. 4b. The feed rate simulator implementation is based on a controlled jerk kinematical model and a discontinuity crossing kinematical model of the couple machine tool and numerical control unit (NCU) [17, 18]. The performance viewer outputs are an ISO block length classification (histogram), an ISO block simulated feed rate classification (histogram), the simulated machining time, and a map of the simulated feed rate on the whole toolpath.

For this work, the feed rate simulation is implemented with the parameters of MIKRON UCP 710 machine tool associated to a Siemens 840D NCU. The characteristics of the NCU are: *x–y–z*-axis maximal feed rate is 30 m/min, *x*-axis maximal acceleration is 2.5 m/s², *y*-axis maximal acceleration is 3 m/s², *z*-axis maximal feed rate is 2 m/s², *x–y*-axis maximal jerk is 5 m/s³, and *z*-axis maximal jerk is 50 m/s³. The following cutting conditions are adopted: 4-mm ball end mill cutting tool, machining deviation fixed to 0.01 mm, cusp height fixed to 0.01 mm, and the machining area sweeping set to upward. Toolpath feed rate simulations are done for 2, 4, and 6 m/min set point.

3 Construction of machining area

The whole area between the two boundaries of the bottom feature is the first machining area to be evaluated. This initial area is the result of the design of the shape, and the different curvatures of the boundaries will spread on toolpaths. The insertion of intermediate curves between the two boundaries can limit this propagation, while using it as a basis for analyzing the influence of curvatures. The association of the intermediate curves and the two boundaries results in the decomposition of the initial zone into multiple machining areas.

3.1 Single machining area

A preliminary decomposition in a single machining area defined between the guides 1 and 2 of the master “bottom feature” is experimented (Fig. 3).

Analysis of the toolpaths generated shows a very limited number (less than 1 % of the total number) of short length

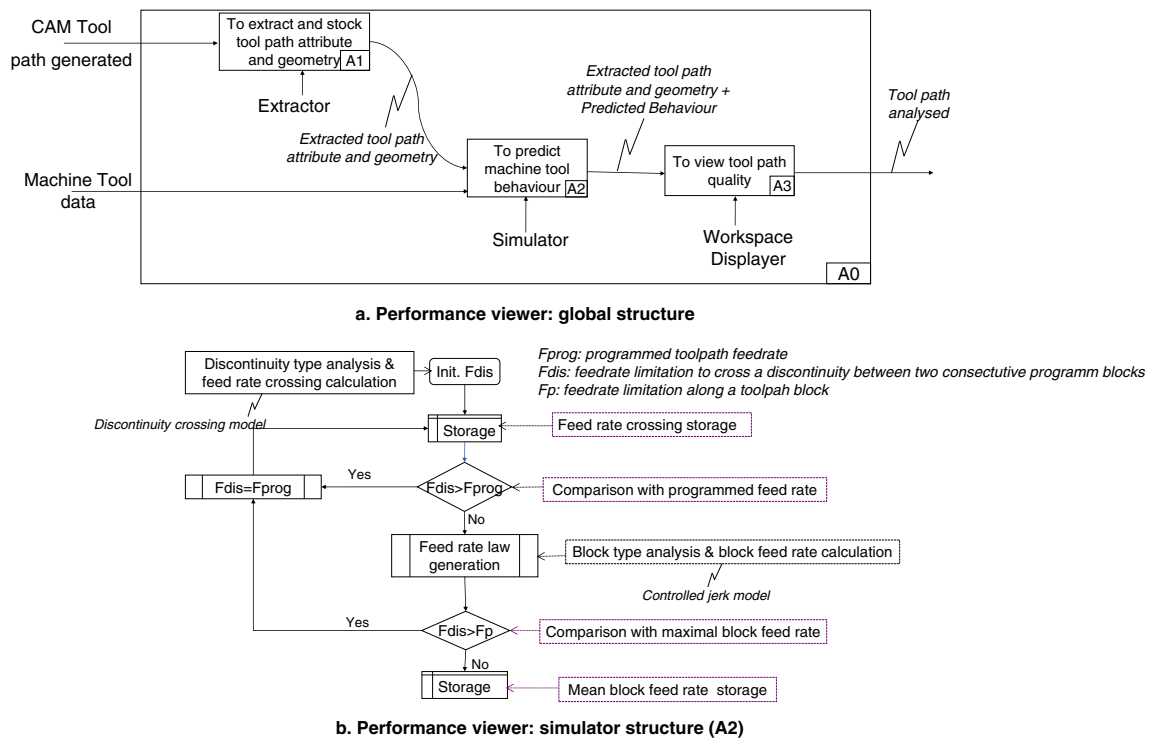


Fig. 4 Performance viewer

machining sequences (Fig. 5b compared to parallel planes strategy (about 40 % of the total number of trajectories, Fig. 5a). Yet, the HSP cannot really be considered better, since the number of entrance/exit in part material is significantly reduced, but the machining time is higher (579 s.) compared to the parallel planes strategy (418 s).

Besides, significant feed rate reductions appear on the central area of the bottom feature (Fig. 6). These reductions derive from the combination of two topological constraints: the bottom feature topology (small radii of curvature) as it

was underlined for the parallel planes strategy (reduction type 1) and the two guide’s topology. Indeed, significant feed rate reductions are induced by spreading of small curvature radii of the two guides (red color in Fig. 6). The guidance curve strategy removes tool entrance/exit paths along boundaries of the bottom feature, but it spreads some local cutting problems on the central area.

To reduce these spreading influences, approach adopted in this work consists in decomposing the bottom feature area in several subareas. Limits, position, and size of each subarea should be defined in order to combine advantages of guidance curves and parallel planes strategies. After the decomposition, each new machining area is a portion of the initial machining feature limited by two curves, from which one at least is different from the boundaries of the bottom feature. Several alternative guidance curves are experimented in order to define the machining area limits, position, and size.

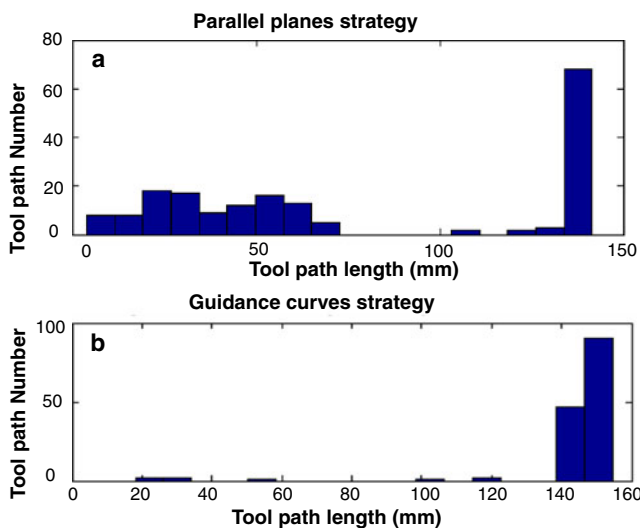
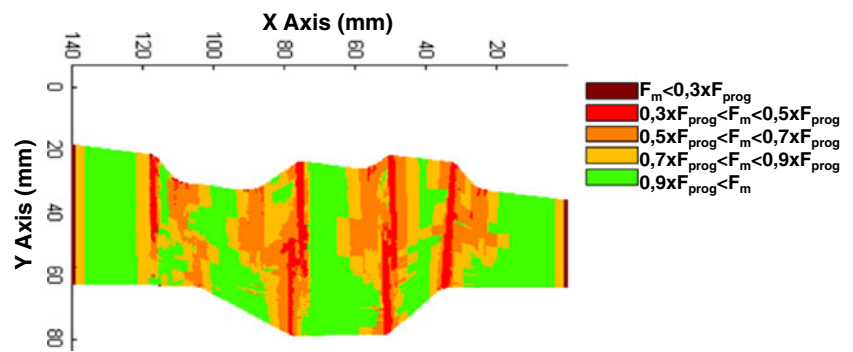


Fig. 5 Trajectories length classification

3.2 Construction of intermediate curves

Curves limiting the subareas are generated between the two boundaries of the bottom feature in an iterative way. To initialize the iteration process, the curve C_{Int_1} is generated between the two boundaries, boundary 1 (B_1) and boundary 2 (B_2), which are the boundaries of the bottom feature. This initialization step principle is illustrated in (Fig. 7a). The two initial boundaries B_1 and B_2 are discretized. The discretization is based on the generation of parallel planes spacing by a step

Fig. 6 Feed rate simulation for guidance curves strategy



P (P_{L_m} in Fig. 7a). Each plane direction is perpendicular to the machining direction of the bottom feature given by topological decomposition explained in [13, 14]. In this work, the machining direction was found parallel to the length “L140” in Fig. 1. Then, the intersecting points, P_{tm1} and P_{tm2} in Fig. 7a, are generated between the two boundaries B_1 and B_2 . According to the principle presented to the Eq. (1), for a given value for K , intermediate points $P_{tm_Int_1}$ are generated in all planes P_{L_m} between P_{tm1} and P_{tm2} . K is a factor introduced in order to represent the topological influence of each boundary B_1 or B_2 on the generation of intermediate curves C_{Int_1} (Fig. 7a).

$$\overrightarrow{Pt_{m1}Pt_{m_Int_1}} = K \times \overrightarrow{Pt_{m1}Pt_{m2}}, \quad K \in]0, 1[\quad (1)$$

Finally, the intermediate curve C_{Int_1} is created as a 5° B-spline curve controlled by points $P_{tm_Int_1}$, 5° B-Spline model implemented in CATIA® V5.

Then, iteration process is based on the generalization of the initialization process for two curves C_a and C_b , which are not intersected (Fig. 7b). Each point $P_{tm_Int_j}$ defining the

intermediate curve is computed using the following Eq. 2.

$$\overrightarrow{Pt_{ma}Pt_{m_Int_j}} = K \times \overrightarrow{Pt_{ma}Pt_{mb}}, \quad K \in]0, 1[\quad (2)$$

Where:

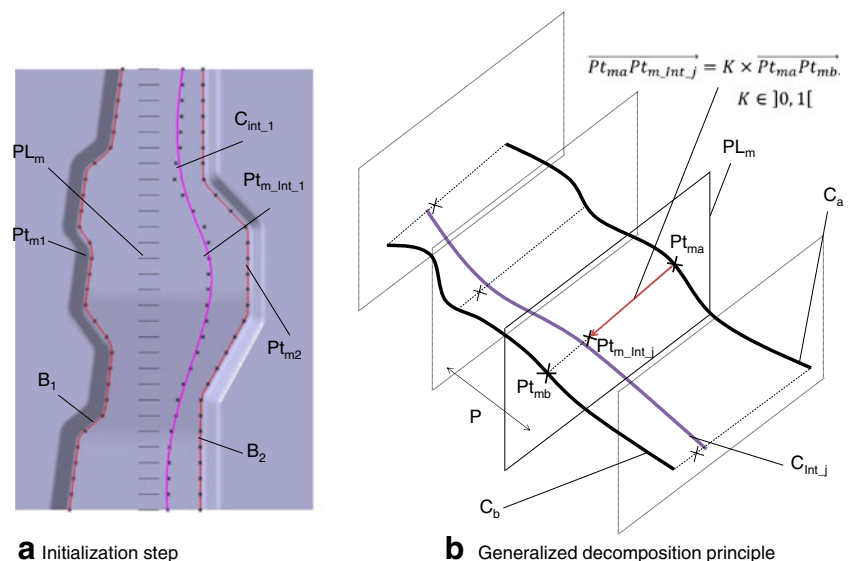
P_{tma} and P_{tmb} are intersection points of P_{L_m} , with the two curves C_a and C_b .

P_{L_m} is one of the discretization planes spacing by a step P and perpendicular to the machining direction of the bottom feature.

For a given value for K , points $P_{tm_Int_j}$ are generated in all planes P_{L_m} . The intermediate curve C_{Int_j} is created as a 5° B-spline curve controlled by points $P_{tm_Int_j}$, 5° B-Spline model implemented in CATIA® V5. K is a factor introduced in order to represent the topological influence of each curve C_a or C_b on the generation of intermediate curves C_{Int_j} .

Then, a net of intermediate curves is generated according to the principle presented below. Each curve C_{Int_j} ($j > 1$) is generated between C_{Int_j-1} and B_1 or B_2 . The iterative process stops when the current intermediate curve C_{Int_j} and B_1 or B_2 are intersecting, i.e., $C_{Int_j} \cap B_1$ or $B_2 \neq \{\emptyset\}$. The last curve

Fig. 7 Intermediate curve building principle



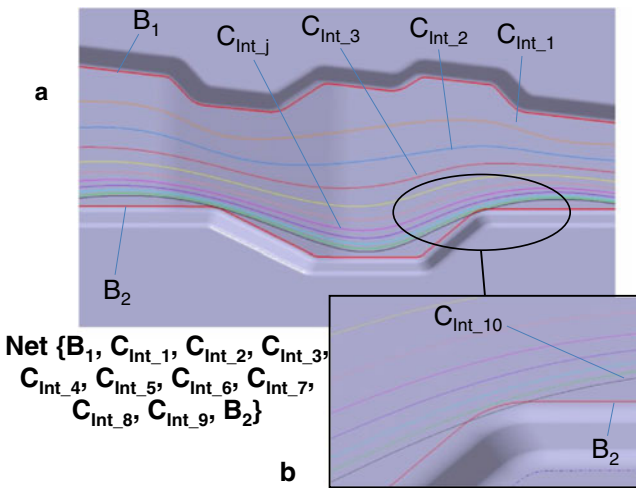


Fig. 8 Curves net building principle for $K=0.25$ and $P=5$ mm

saved is $C_{Int_{j-1}}$. Thus, the net of curves generated is $(B_1, C_{Int_1}, \dots, C_{Int_{j-1}}, B_2)$. For the example presented in Fig. 8a, the iterative process is applied from B_1 to B_2 , $C_{Int_{10}}$ intersects B_2 (Fig. 8b), thus, C_{Int_9} is the last curve generated in the net.

The composed machining area is defined as the association of elementary machining areas covering the global machining area of the bottom feature. Each elementary machining area is limited by two consecutive curves of the net generated.

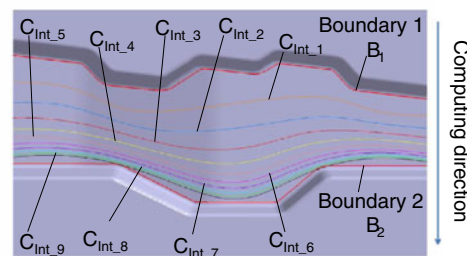
3.3 Construction of multiple machining area

3.3.1 Boundary direction machining area

The first type of decomposition is carried out with two nets of intermediate curves: from B_1 to B_2 and from boundary 2 to boundary 1. For $K=0.25$, nine intermediate curves from B_1 to B_2 are generated and illustrated in Fig. 9. Based on these

Fig. 9 Composed machining areas ($K=0.25$)

Curves net built
 $\{B_1, C_{Int_1}, C_{Int_2}, C_{Int_3}, C_{Int_4}, C_{Int_5}, C_{Int_6}, C_{Int_7}, C_{Int_8}, C_{Int_9}, B_2\}$



Machining areas	
$M_{A1} = \{B_1, C_{Int_1}\} \cup \{C_{Int_1}, B_2\}$	$M_{A4} = \{B_1, C_{Int_1}\} \cup \{C_{Int_1}, C_{Int_2}\} \cup \{C_{Int_2}, C_{Int_3}\} \cup \{C_{Int_3}, C_{Int_4}\} \cup \{C_{Int_4}, B_2\}$
$M_{A2} = \{B_1, C_{Int_1}\} \cup \{C_{Int_1}, C_{Int_2}\} \cup \{C_{Int_2}, B_2\}$	$M_{A5} = \{B_1, C_{Int_1}\} \cup \{C_{Int_1}, C_{Int_2}\} \cup \{C_{Int_2}, C_{Int_3}\} \cup \{C_{Int_3}, C_{Int_4}\} \cup \{C_{Int_4}, C_{Int_5}\} \cup \{C_{Int_5}, B_2\}$
$M_{A3} = \{B_1, C_{Int_1}\} \cup \{C_{Int_1}, C_{Int_2}\} \cup \{C_{Int_2}, C_{Int_3}\} \cup \{C_{Int_3}, B_2\}$	$M_{A6} = \{B_1, C_{Int_1}\} \cup \{C_{Int_1}, C_{Int_2}\} \cup \{C_{Int_2}, C_{Int_3}\} \cup \{C_{Int_3}, C_{Int_4}\} \cup \{C_{Int_4}, C_{Int_5}\} \cup \{C_{Int_5}, C_{Int_6}\} \cup \{C_{Int_6}, B_2\}$
$M_{A7} = \{B_1, C_{Int_1}\} \cup \{C_{Int_1}, C_{Int_2}\} \cup \{C_{Int_2}, C_{Int_3}\} \cup \{C_{Int_3}, C_{Int_4}\} \cup \{C_{Int_4}, C_{Int_5}\} \cup \{C_{Int_5}, C_{Int_6}\} \cup \{C_{Int_6}, C_{Int_7}\} \cup \{C_{Int_7}, B_2\}$	$M_{A8} = \{B_1, C_{Int_1}\} \cup \{C_{Int_1}, C_{Int_2}\} \cup \{C_{Int_2}, C_{Int_3}\} \cup \{C_{Int_3}, C_{Int_4}\} \cup \{C_{Int_4}, C_{Int_5}\} \cup \{C_{Int_5}, C_{Int_6}\} \cup \{C_{Int_6}, C_{Int_7}\} \cup \{C_{Int_7}, C_{Int_8}\} \cup \{C_{Int_8}, B_2\}$
	$M_{A9} = \{B_1, C_{Int_1}\} \cup \{C_{Int_1}, C_{Int_2}\} \cup \{C_{Int_2}, C_{Int_3}\} \cup \{C_{Int_3}, C_{Int_4}\} \cup \{C_{Int_4}, C_{Int_5}\} \cup \{C_{Int_5}, C_{Int_6}\} \cup \{C_{Int_6}, C_{Int_7}\} \cup \{C_{Int_7}, C_{Int_8}\} \cup \{C_{Int_8}, C_{Int_9}\} \cup \{C_{Int_9}, B_2\}$

intermediate curves, the machining area between B_1 and B_2 is decomposed in an iterative way: $M_{A1} = \{B_1, C_{Int_1}\} \cup \{C_{Int_1}, B_2\}$, $M_{A2} = \{B_1, C_{Int_1}\} \cup \{C_{Int_1}, C_{Int_2}\} \cup \{C_{Int_2}, B_2\}$, and for $j=3$ to 9 $M_{Aj} = \{B_1, C_{Int_1}\} \cup \{C_{Int_1}, C_{Int_2}\} \cup \dots \cup \{C_{Int_{j-1}}, C_{Int_j}\} \cup \dots \cup \{C_{Int_j}, B_2\}$. Machining simulation of these nine decomposed areas allows analyzing the spreading of boundary 1's topology constraints.

The spreading influence is analysed for $K=0.75$, and the decomposition process is carried out also in the second direction from B_2 to B_1 . All the machining areas decomposition type 1 experimented are presented in Table 1.

3.3.2 Median curve machining area

The second type of decomposition is carried out with a predecomposition into two machining areas at the initialization step. A median curve (C_{med}) is generated according to the intermediate curve principle with $K=0.5$. This value is chosen in order to expect the same influence of the two boundaries in each predecomposed machining area. Intermediate curves' net are generated in each two predecomposed area: in one hand from B_1 and B_2 to the median curve, and in the other hand from the C_{med} to B_1 and B_2 (Fig. 10). The composed machining areas are built based on the same principle presented previously. For $K=0.5$, six elementary machining areas are generated, three areas from the median curve C_{med} to B_1 and three other areas from C_{med} to B_2 (illustrated in Fig. 10).

All the composed machining areas generated are presented in Table 2. The number of intermediate curves and their position with respect to the boundaries are defined with: $K=0.25$, $K=0.5$, and $K=0.75$. Besides, the number of control points used to generate intermediate curves is also defined through different step values: $P=5$, $P=10$, and $P=20$ mm between two consecutive control points.

Table 1 Composed machining areas type 1

Curves net characteristics				Number of elementary machining areas
P	Building direction	K	C _{Int} number	
5 mm	Boundary 1 to Boundary 2	0.25	9	2,3, 4, 5, 6, 7, 8, 9, 10
		0.75	1	2
	Boundary 2 to Boundary 1	0.25	9	2,3, 4, 5, 6, 7, 8, 9, 10
		0.75	1	2

4 Results and discussion

4.1 Analysis of boundary direction machining area

For the machining area created with $K=0.75$ (illustrated in Fig. 11b) according to the building direction boundary 1 to boundary 2, the machining time is equal than those of the single machining area (between boundaries 1 and 2 illustrated in Fig. 11a), and tool path lengths are higher than those of the single machining area. As might be expected, the decomposition of the bottom surface in two elementary machining areas (Fig. 11b) involves some limiting feed rate reductions around the intermediate curve compared with the single machining area (Fig. 11a). This observation is reinforced by the classification of blocks according to the feed rate. The number of short toolpaths does not change, but their feed rates remain as low as for the single machining area. The addition of intermediate curves seems relevant to limit only feed rate reductions.

When the initial area is decomposed in 2 elementary areas with $K=0.25$ (M_{A1} equivalent to $K=0.75$ in the direction

from boundary 2 to boundary 1), machining time, tool paths length, and block’s number in each feed rate class are equivalent. Some feed rate reductions are localized around the intermediate curve compared with the single machining area, as it is previously observed.

For the composed machining areas obtained for $K=0.25$, machining time and toolpath length remain higher than those of the single machining area. As might be expected, values of these two criteria increase with the number of elementary machining areas, i.e., the addition of intermediate curves imply an increase of machining time and toolpath length. Yet, addition of intermediate curves limits feed rate reductions compared with the single machining area. In this case, remaining feed rate reductions are reflected towards the second boundary in the construction direction of intermediate curves. Figure 12 shows the comparison between machining areas M_{A1} and M_{A9} . The reflection of feed rate reductions towards boundary 2 is clearly visible (area 2 in Fig. 13a and b) for the decomposition M_{A9} (ten elementary machining areas). Feed rate reductions appearing in the first elementary machining area (area 1 between B_1 and C_{Int1} in

Fig. 10 Composed machining areas ($K=0.5$)

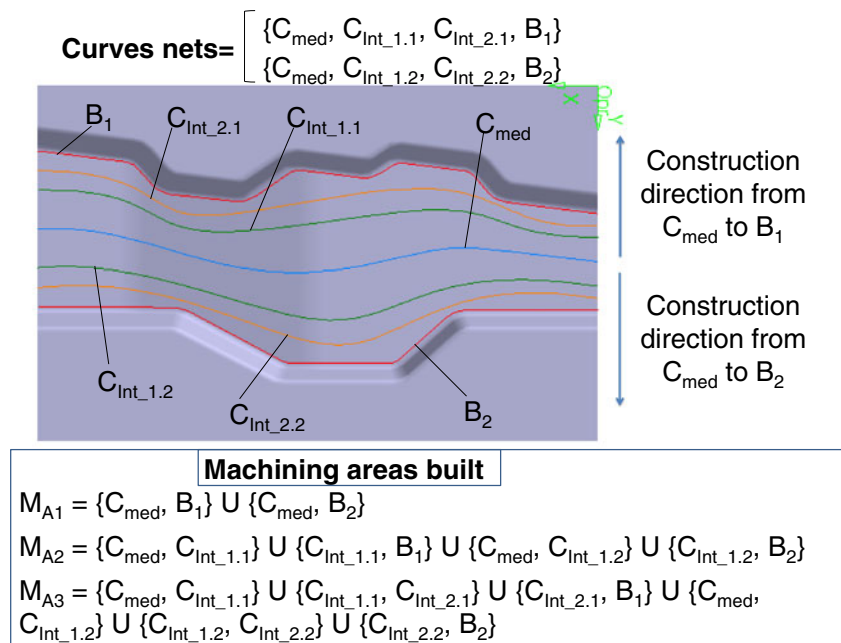


Table 2 Composed machining areas built on curves net with median

Curves net characteristics				Number of elementary machining areas
P	Building direction	K	C_{Int} number	
5, 10, 20 mm	Boundary 1 to C_{med} and Boundary 2 to C_{med}	0.25	13	2, 4, 6, 8, 10, 12, 14
		0.5	5	2, 4, 6
		0.75	3	2, 4
	C_{med} to Boundary 1 and C_{med} to Boundary 2	0.25	13	2, 4, 6, 8, 10, 12, 14
		0.5	5	2, 4, 6
		0.75	3	2, 4

Fig. 13a and b) require the construction of additional intermediate curves between B_1 and C_{Int1} for the building direction B_1 to B_2 . Improvement made by this construction of additional curves is observed when the construction direction changes from B_2 to B_1 (area 1 between B_2 and C_{Int1} in Fig. 13c).

The generation of elementary areas by construction of intermediate curves between the two boundaries B_1 and B_2 reflects feed rate reductions towards the second boundary according to the construction direction. The first elementary area generated integrating the first boundary is too large to give the same result as that observed close to the second boundary. For this reason, the construction of intermediate curves in the two directions must be combined. This combination requires the division of the single machining area (between B_1 and B_2) into two areas with a main intermediate curve. The shape and the position of this main intermediate curve have to be defined.

The comparison between two elementary areas generated for $K=0.25$ (M_{A1}) or $K=0.75$ shows that the machining time and the number of feed rate reductions are not affected by the position of the intermediate curve with respect to the boundaries. Yet, curves limiting elementary machining areas will generate feed rate reductions.

Addition of several intermediate curves implies that machining time increases (until 20 % for $K=0.25$),

whereas feed rate reductions are very limited. This observation can be explained by the evolution of curvature radii (from small to soft radii) on the limits of the elementary machining areas. The number of intermediate curves might be maximized to limit feed rate reductions, but this maximization will increase the machining time. The number of intermediate curves and their proximity to the boundaries must be analysed to find the better balance between feed rate reductions (parts geometrical and mechanical requirements) and machining time (productivity).

4.2 Analysis of median curve machining area

In the first step of these experiments, elementary areas are generated for a given value for K by addition of intermediate curves from median curve to, respectively, B_1 and B_2 . As it might be expected, feed rate reductions are reflected towards each boundary, and the machining time increases with the number of intermediate curves.

When construction directions of intermediate curves are inverted (from each boundary to median curve), the machining areas created limit the feed rate reductions in the elementary areas closed to the boundaries. The number of elementary machining areas increases with the machining time, but it does not affect feed rate reductions.

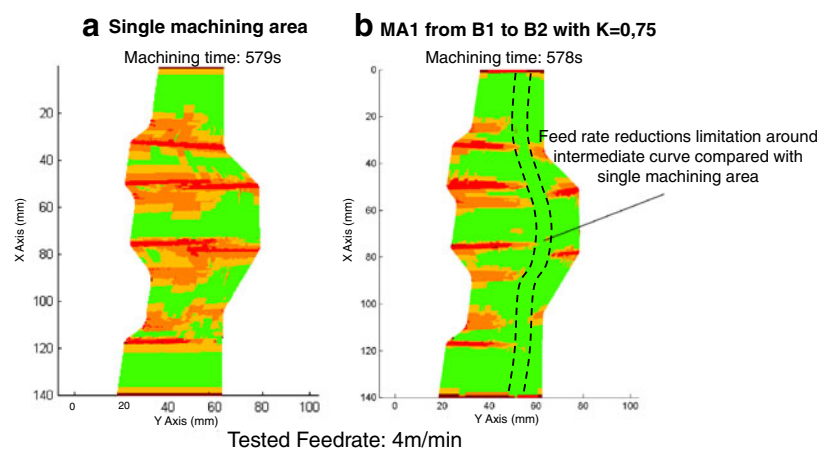
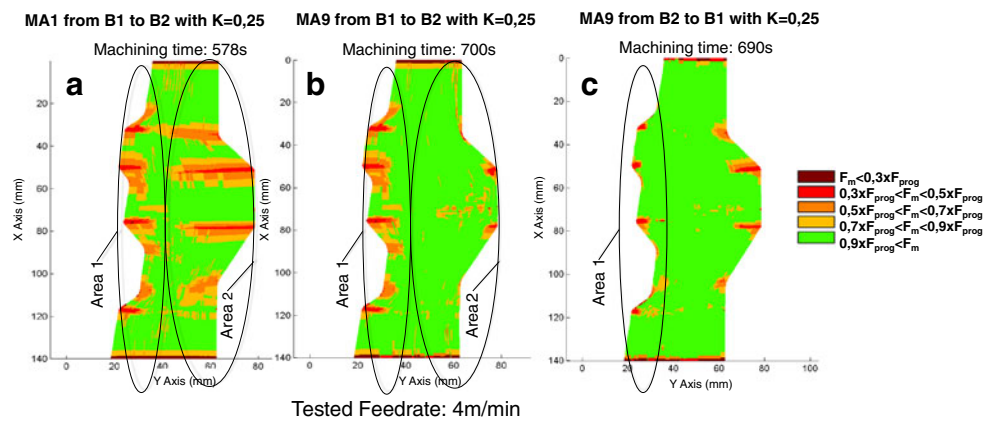
Fig. 11 Feed rate simulations for single machining area and composed machining area MA1 ($K=0,75$)

Fig. 12 Feed rate simulations for composed machining areas M_{A1} and M_{A9}



A first conclusion can be made: the construction of intermediate curves gives best results from the median curve to each boundary for the limitation of feed rate reductions. The number of intermediate curves increases with the machining time, as it was previously observed in the first experiments.

Feed rate simulations for a decomposition of the single area into four elementary areas are presented in Fig. 13. The comparison of these three simulations highlights a better limitation of feed rate reductions when elementary areas are positioned more close to the boundaries for $K=0.75$ (Fig. 13c). In these three cases, the machining time remains equivalent. The size of the first elementary machining area for $K=0.75$ (Fig. 13c) is greater than for $K=0.5$ (Fig. 13b), itself being greater than $K=0.25$ (Fig. 13a).

Feed rate simulation for the decomposition of the single machining area into 4 elementary areas for $K=0.75$ (Fig. 14a) is compared to the one realized for the decomposition into 14 elementary areas for $K=0.25$ (Fig. 14b). For each one of these simulations, several elementary machining areas are localized close to the boundaries. The number of elementary machining areas in the central area is greater for $K=0.25$ than for $K=0.75$. When considering feed rate reductions, results are equivalent for the two decompositions. Yet, the machining time is greater for $K=0.25$.

A second conclusion can be made: to limit feed rate reductions for a same number of elementary machining areas

and a same (or equivalent) machining time, it is necessary to localize elementary machining areas close to the boundaries. The number of elementary machining areas, i.e., the number of intermediate curves close to boundaries increases with the machining time without any significant change for feed rate reductions. According to experiments carried out, the decomposition of the single machining area into four elementary areas is the most relevant with a value for K close to 0.75.

As last conclusion concerning the intermediate curve smoothing, the variation of the step P does not have a significant influence on the results already observed. However, it is advisable to retain its smallest value than possible, which can be set to 5 mm.

4.3 Definition of guidance curves

Analysis of the experiments performed shows that the appropriate solution for the “bottom machining” feature proposed in this work is to decompose the single machining area of the bottom machining feature in four elementary areas generated with three intermediate curves. The first intermediate curve is the C_{med} generated between the boundaries with $K=0.5$ according to the principle presented in this paper. The two others intermediate curves (C_{Int_1} and C_{Int_2}) are generated with $K=0.75$ between the C_{med} and each boundary (B_1 and B_2). Based on the experiments, a first

Fig. 13 Feed rate simulations for composed machining areas with four elementary areas

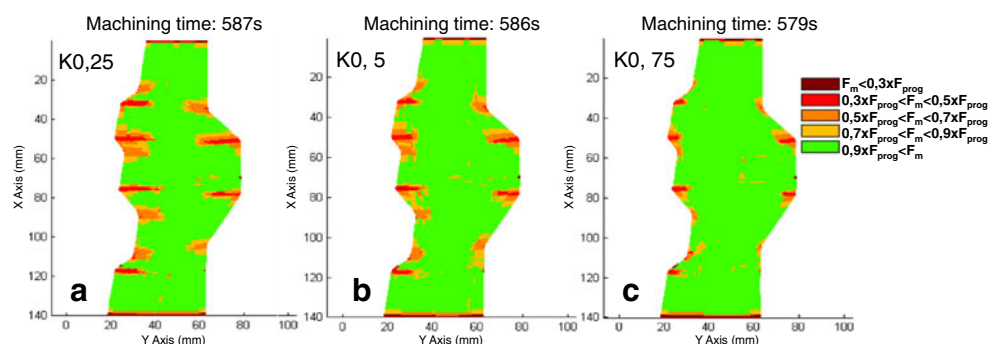
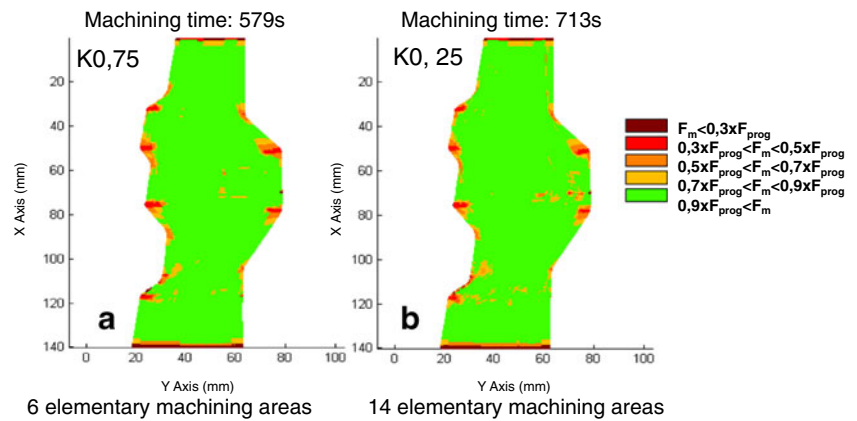


Fig. 14 Feed rate simulations for more than four elementary areas



definition of guidance curves can be proposed in four steps for a given cavity:

- Step 1 Generate the C_{med} between the boundaries B_1 and B_2 with $K=0.5$. This median curve separates the initial machining area into two subareas.
- Step 2 Determine the appropriate step P for smoothing intermediate curves. Indeed, the discretization of the two guidance curves with the initial step set to 5 mm can lead to very few points or no points, when the radius of curvature is very small. The projection of the inflection points of the two guidance curves on a line parallel to the machining direction makes it possible to set the suitable value of the step or to adapt it along the machining direction.
- Step 3 For each subarea limited by two guidance curves, which correspond to the median curve and one boundary B_1 or B_2 , generate intermediate curves with $K=0.75$, starting from the guidance curve, which smallest radius of curvature is greatest. A line as a guidance curve is still considered as the starting curve, and when the two guidance curves are lines, it is not necessary to generate intermediate curves.
- Step 4 Generate and simulate tool paths for all machining areas created. The value of K can be increased or decreased slightly to see if there is improvement.

The first method proposed to define the guide curves provides assistance for machining specialists. The method will be generalized based on further experiments being conducted. This generalization will be communicated later.

5 Conclusion

The machining of complex shapes is often based on two conventional strategies: parallel plane and Z level. Tool paths generated with these conventional strategies for a bottom

machining feature have many feed rate reductions, especially when both boundaries have a lot of curvatures and are not parallel. Experimental approach presented in this paper is aimed to highlight the influence of the curvatures towards a suitable decomposition of the machining area limited by both boundaries. It also introduces one of the uncommon methods of implementation of the curve guidance machining strategy available in CAD/CAM software.

The bottom feature usually present in the cavities of complex shape dies is part of the experimental setup. Difficulties of generating tool paths often encountered with this machining feature were first analyzed towards parallel planes strategy before the decomposition of the machining area. Feed rate reductions highlighted in the scope of the first analysis are completed by the high-performance evaluation, which is carried out by means of the computation of toolpaths' length for each ISO block extracted from the machining program and sent to the machine tool. Other components of high-performance as the machining time and the geometrical allowance are also evaluated, but they are not presented because their variations are not significant. Application of the approach to other types of open machining features (nonclosed boundary) is trivial, when the two limit curves are identified and extracted.

The decomposition of the machining area is achieved through the construction of intermediate curves between the two boundaries. At first, a series of points, proportionally spaced from both boundaries are created before they are approximated to create each curve. The ratio of the distances between points and a given boundary reflects the influence of its curvatures on the intermediate curve. The ratio of the distances is the first key parameter of the proposed approach. To prevent the spread of the influence of the curvatures of one boundary to the other boundary, the median curve was finally created. It shares the machining area in two portions before the decomposition.

Machining areas evaluated are constructed by combining intermediate curves created before. Results were

analysed at several levels. First, it was shown that increasing the number of intermediate curves tends to limit the feed rate reductions, while also increasing the machining time. Then, it was noted that the introduction of the median curve leads to a significant decrease in feed rate reductions, when the intermediate curves are constructed from this curve to the boundaries. Finally, the observations show that the positioning of the machining areas (intermediate curves) closest to the boundaries gives better results, and the variation of the curves smoothing step P has no significant influence on the results. Based on the results, a method for defining guidance curves in four steps was proposed. The generalization of the method as well as additional experiments will be communicated.

References

- Kranjnik P, Kopac J (2004) Modern machining of die and mold tools. *J Mater Process Technol* 157–158:543–552
- Kecelj B, Kopac J, Kampus Z, Kuzman K (2004) Speciality of HSC in manufacturing of forging dies. *J Mater Process Technol* 157–158:536–542
- Anderberg S, Beno T, Pejryd L (2009) CNC machining process planning productivity – a qualitative survey, In: *Proceedings of The International 3rd Swedish Production Symposium, SPS 09*. - 978-91-633-6006-0; s. 228–235
- Flutter A, Todd J (2001) A machining strategy for tool making. *Comput Aided Des* 33:1009–1022
- Rech J, Hamdi H, Valette S (2008) Workpiece surface integrity. In: Davim JP (ed) *Machining: fundamentals and recent advances*. Springer, London, pp 59–96
- Toh CK (2005) Design, evaluation, and optimization of cutter path strategies when high-speed machining hardened mold and die materials. *Mater Des* 26:517–533
- Axinte DA, Dewes RC (2002) Surface integrity of hot work steel after high-speed milling-experimental data and empirical models. *J Mater Process Tech* 127:325–335
- Kalvoda T, Hwang YR (2009) Impact of various ball cutter tool positions on the surface integrity of low carbon steel. *Mater Des* 30:3360–3366
- Kang MC, Kim KK, Lee DW, Kim JS, Kim NK (2001) Characteristics of inclined planes according to the variation of cutting direction in high-speed ball-end milling. *Int J Adv Manuf Technol* 17:323–329
- Ramos AM, Relvas C, Simoes JA (2003) The influence of finishing milling strategies on texture, roughness, and dimensional deviations on the machining of complex surfaces. *J Mater Process Technol* 136:209–216
- Guo YB, Li W, Jawahir IS (2009) Surface integrity characterization and prediction in machining of hardened and difficult-to-machine alloys: a state-of-art research review and analysis. *Mach Sci Technol* 13:437–470
- Guillemot N, Mawussi BK, Lartigue C, Billardon R (2013) A first approach to characterize the surface integrity generated by ball-end finishing milling. *Int J Adv Manuf Technol* 64:269–279
- Tapie L, Mawussi BK (2008) Decomposition of forging die for high speed machining, In *IDMME -Virtual concept conference 2008*, Beijing, China
- Mawussi KB, Tapie L (2011) A knowledge base model for complex forging die machining. *Comput Ind Eng* 61:84–97
- Ding S, Mannan MA, Poo AN, Yang DCH, Han Z (2003) Adaptive isoplanar tool path generation for machining of free-form surfaces. *Comput Aided Des* 35:141–153
- Ding S, Mannan MA, Poo AN, Yang DCH, Han Z (2005) The implementation of adaptive isoplanar tool path generation for the machining of free-form surfaces. *Int J Adv Manuf Technol* 26:852–860
- Tapie L, Mawussi BK, Anselmetti B (2007) Circular tests for HSM machine tools: bore machining application. *Int J Mach Tool Manuf* 47:805–819
- Tapie L, Mawussi BK, Anselmetti B (2007) Machining strategy choice: performance viewer. In: Tichkiewitch S, Tollenaere M, Ray P (eds) *Advances in integrated design and manufacturing in mechanical engineering II*. Springer, Dordrecht, Netherlands, pp 343–356